

Hybridization of the 3d states of transition metals with the states of the ZnS matrix

K. Lawniczak-Jablonska,* R. C. C. Perera, J. H. Underwood, and E. M. Gullikson
Center for X-ray Optics, Lawrence Berkeley Laboratory, Berkeley, California 94720

R. J. Iwanowski

Institute of Physics Polish Academy of Science, Al. Lotnikow 32/46, 02 668 Warsaw, Poland

(Received 5 August 1996; revised manuscript received 26 December 1996)

The near-edge soft x-ray absorption spectra of $Zn_{1-x}M_xS$ compounds (where M is Mn, Fe, Co, and Ni, and x ranges to the solubility limit) have been obtained by measuring the total electron yield (photoelectron, Auger and secondary) from the sample in an ultrahigh vacuum (UHV) sample chamber using x-rays from beam line 6.3.2, a bending magnet beamline at the Advanced Light Source (ALS). The high spectral resolution of the beamline in the 50–1000 eV region allowed detailed measurements of S- $L_{2,3}$ and transition metal L_3 absorption spectra. The study of d and s antibonding states in $Zn_{1-x}M_xS$ compounds provided evidence that 3d states of transition metals participate in the formation of ionic-covalence bonding between M-S. Furthermore, it was found that the ability of 3d electrons to participate in bonding decreases with increasing 3d orbit filling. As the 3d orbit becomes more closed, the 3d electrons assume a more corelike character. The evidence of these behaviors can be seen in the metal and sulfur L absorption spectra as well as in the charge transfer values calculated from the energy shifts in transition metal K edges. These findings provided an explanation for the drastic decrease in the solubility of these particular metals in the ZnS matrix. [S0163-1829(97)09716-6]

I. INTRODUCTION

The current interest in the technology and properties of ternary alloys results from the increasing expectation by the electronic industry that these materials will have useful physical, optical, mechanical, and chemical properties for future electronic devices. The alloying of elements makes it possible, in many cases, continuously to change the properties of materials, for example the lattice parameters, energy gap, conductivity, magnetic moment, plasticity, corrosion endurance, etc... In particular, the II-VI wide band-gap materials have recently attracted attention, as heterostructures grown from them are potential candidates for blue-green light-emitting devices and diode lasers.^{1,2} The scientific and commercial interest in these materials reaches back to at least several decades. ZnS in particular has long been used as a host material in phosphors, where doping by transition metal elements produces high cathodoluminescence efficiencies. In spite of the wide commercial value of ZnS based materials, many of their physical properties still lack proper explanation.

In II-VI compounds, the partial substitution of a cation by a magnetic ion of a transition element should result in hybridization of the 3d states with the sp band states of the host semiconductor. This will inevitably lead to modification of the crystalline, electronic, and magnetic structures. EXAFS (extended x-ray-absorption fine structure) studies have demonstrated the existence of two different bond lengths between different cations and the anion.³⁻⁶ Evidence of modification of the electronic structure has been observed by photoelectron, reflectivity, and x-ray-absorption near-edge structure studies⁷⁻¹⁰ of these compounds.

Inner shell absorption spectroscopy provides a useful means of electronic structure analysis in a wide variety of systems. Resulting from the atomic and symmetry selectiv-

ity, the soft x-ray absorption technique offers a unique opportunity to directly measure the site-selective energy distribution of the unoccupied d states of these compounds. The degree of hybridization of the 3d states and its interaction with the host material band states has been a subject of many discussions.⁹⁻¹² Nevertheless, until now it has not been possible to probe the distribution of d states around the given atom with energy resolution sufficient to recognize the degree of hybridization between states of different atoms. The evidence of d -states hybridization was not observed in a previous paper by Li *et al.*,¹² probably due to insufficient energy resolution.

In the present paper we report the near-edge soft x-ray absorption spectra from $Zn_{1-x}M_xS$ compounds, where M is Mn, Fe, Co, and Ni, and x ranges from very low concentrations to the solubility limit. Specifically, the S- $L_{2,3}$ and the L_3 edges of transition metals were measured, and the results are discussed. The details of the crystal growth and sample characterization along with that of the complementary investigations of the zinc, sulfur, and transition metal K absorption spectra were presented elsewhere.⁹

II. EXPERIMENTAL

BL 6.3.2, an entrance-slitless bend magnet beam line¹³ at the Advanced Light Source (ALS) operating in the 50–1000 eV energy region is equipped with a Hettrick-Underwood type varied line space grating monochromator and various mechanical design features resulting in high performance in energy resolution, throughput, stability, and ease of operation. The resolving power of the monochromator $E/\Delta E$ at the $L_{2,3}$ edge of S is about 1700, and at the transition metal L_3 edges of Mn through Ni are between 1000 and 1500. This energy resolution was sufficient to distinguish the fine changes in the spectra as a function of transition metal con-

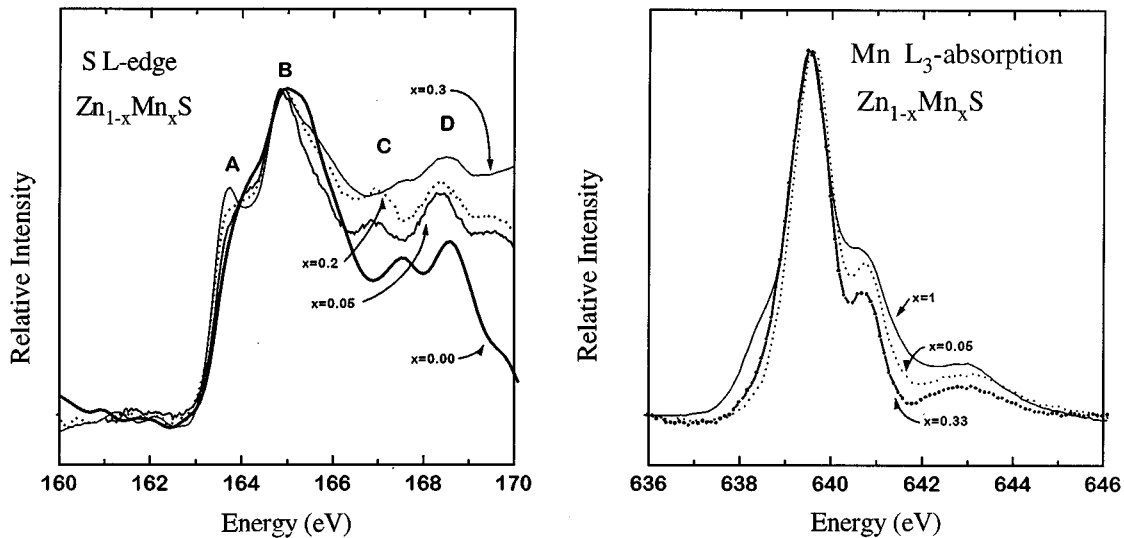


FIG. 1. The Mn- L_3 spectra normalized at the maximum intensity, $x=0.05$ (dotted line), $x=0.33$ (bold line), $x=1.0$ (thin line), and the S- $L_{2,3}$ absorption spectra normalized at the maximum intensity, $x=0.0$ (bold line), $x=0.05$ (middle line), $x=0.2$ (dotted line), $x=0.3$ (thin line) of $Zn_{1-x}Mn_xS$.

tent. Increasing the resolving power up to about 4000 did not result in resolving new structures or narrowing of peaks in the absorption spectra but significantly decreased the signal intensity.

We have measured the high resolution x-ray absorption spectra at the L_3 edges of transition metals and at the $L_{2,3}$ edge of sulfur in $Zn_{1-x}M_xS$ starting from very low concentration ($x=0.01$) to the solubility limit. The spectra presented in this work are the ratio of I/I_0 . To our knowledge these spectra represent the most precise measurements of these compounds at the $L_{2,3}$ edge of sulfur. In recently published data for ZnS ¹² structural details observed in our measurements were not detected. The powder samples were spread on to indium foil, and the I component of the absorption spectra presented in this paper were obtained by step scanning the monochromator and measuring the total electron yield (photoelectron, Auger, and secondary) from the sample (foil) in a high vacuum (HV) sample chamber. Since the sample thickness was larger than the electron escape depths (~ 100 Å), the absorption spectra obtained by this method are not distorted by the inhomogeneity (roughness) of the sample, the so called "thickness effect." This was illustrated in the comparison of N-K absorption spectra of GaN obtained from a powder sample, a single crystal, and an epitaxial film presented elsewhere.¹⁴ The disadvantages of using the total electron yield are that measurements are surface sensitive and it is not possible to obtain absolute absorption cross-section values. But, any appreciable C-K and O-K absorption features from these dilute magnetic semiconductor (DMS) samples were not observed indicating any possible surface contamination in these samples. The intensity of the incoming radiation I_0 was monitored by the photocurrent generated in the gold mesh positioned immediately before the sample. No structure in the I_0 was detected in the high-energy region. Resulting from the design of the beamline (mirror and grating angles) the photon flux above 1000 eV is extremely low. Therefore, no filters or any other high-order suppression was used for metal L absorption measure-

ments presented in this paper. In the case of sulfur L absorption measurements, an order sorter to suppress the high-order radiation,¹³ positioned before gold mesh (I_0), was used and no contribution from higher orders were detected during these measurements.

III. RESULTS AND DISCUSSION

Due to the dipole selection rules, the intensity of L absorption spectral features provides a measure of the 3d and 4s state distributions in the conduction band and allows us to measure directly the degree of antibonding state hybridization at the site of different atoms. The L_3 absorption features result from the transitions of electrons from the $2p_{3/2}$ atomic level to the final states in the conduction band. These transitions are localized on the emitting atom, providing the site selective densities of states. In Figs. 1–4, the transition metals (M) L_3 absorption spectra of the $Zn_{1-x}M_xS$ (where M is Mn, Fe, Co, and Ni) are presented. For direct comparison, the L_3 absorption spectra from related monochalcogenides (labeled $x=1.0$) are also shown in the same figure. The fine structure in these spectra are well resolved. All the spectra presented in this work are normalized to the peak intensity.

The S- $L_{2,3}$ spectra of the corresponding $Zn_{1-x}M_xS$ for various x values are also shown in Figs. 1–4. Even though the S- $L_{2,3}$ spin orbit splitting is approximately 1 eV, the S- L_2 and - L_3 are not well separated in these spectra because of the inherent width of these absorption features. For direct comparison, the S- $L_{2,3}$ absorption spectrum of ZnS (labeled $x=0.0$) measured under the same conditions is also shown in Figs. 1–4.

These compounds (except the Mn containing compounds) exist in the NiAs crystal structure (type B13) if they are binary compounds, and in the zinc-blende structure if they are ternary compounds. The Mn containing binary compounds are in NaCl crystalline structure (type B 1), whereas the ternary compounds are in a wurzite structure. In both structures each atom in a binary and ternary compound is

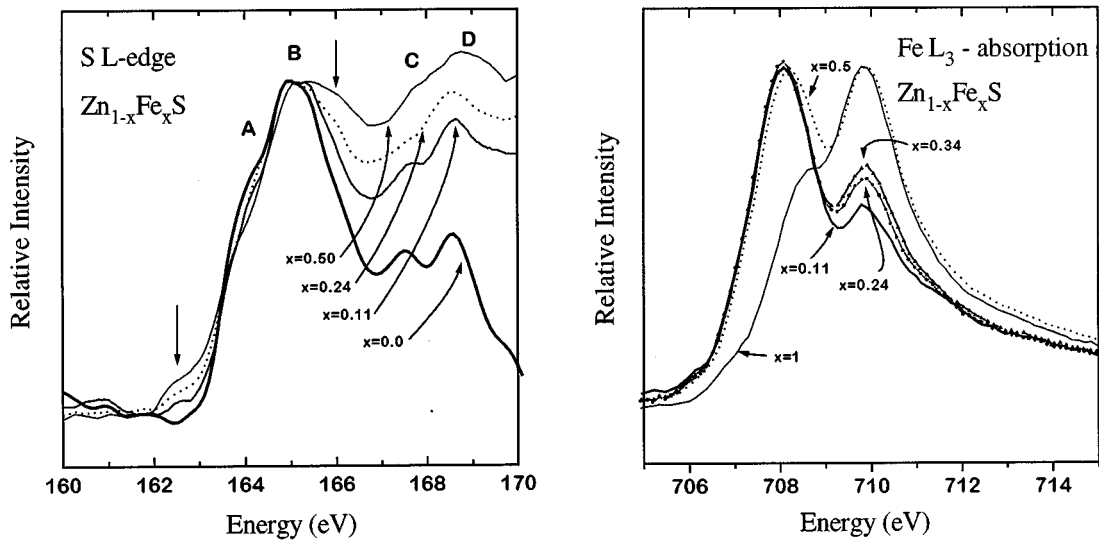


FIG. 2. The Fe-L₃ spectra normalized at the maximum intensity, $x=0.11$ (bold line), $x=0.24$ (dot and continuous line), $x=0.34$ (triangle and continuous line), $x=0.50$ (dotted line), $x=1.0$ (thin line), and the S-L_{2,3} absorption spectra normalized at the maximum intensity, $x=0.0$ (bold line), $x=0.11$ (middle line), $x=0.24$ (dotted line), $x=0.50$ (thin line) of Zn_{1-x}Fe_xS.

surrounded by six or four nearest neighbors, respectively.

The Mn-L₃ spectra shown in Fig. 1 are very similar except that the pre-edge structure observed in the MnS is not observed in these ternary compounds. For clarity of presentation, only spectra from samples with the smallest ($x=0.05$) and largest ($x=0.33$) content of Mn are shown. The spectra from ternary compounds have the well distinguished three-peak structure, suggesting the existence of three subbands in the main $3d-4s$ antibonding band. The energy difference between the first peak and second and third peaks are 1.4 eV and 3.6 eV, respectively. The energy position of these peaks resulting from the subbands do not change significantly with the change in Mn content of these ternary alloys; only a 0.2 eV shift of the low-energy edge between the spectra with the highest and lowest content of Mn was observed. Furthermore, the intensities of the second and third absorp-

tion features decrease with increasing Mn content, suggesting that the $3d$ antibonding states are concentrated near the main subband.

As seen from the S-L_{2,3} absorption spectra of Zn_{1-x}Mn_xS presented in Fig. 1, substitution of only 5% of Zn atoms by Mn atoms have already changed the shape of the sulfur edge. As the concentration of Mn increases, the intensity of the first absorption feature (labeled A) increases and shifts slightly to the low energy, whereas the main peak (labeled B) becomes narrower. The energy positions of peaks C and D also change. These energy shifts indicate that as the Mn content increases, the amount of sulfur states that hybridize with the Mn states also increases. The hybridized states are shifted to the low energy as in the case of Mn $3d$ states. This is direct evidence that the $3d$ Mn states participate in the formation of the chemical bond and hybridize with the

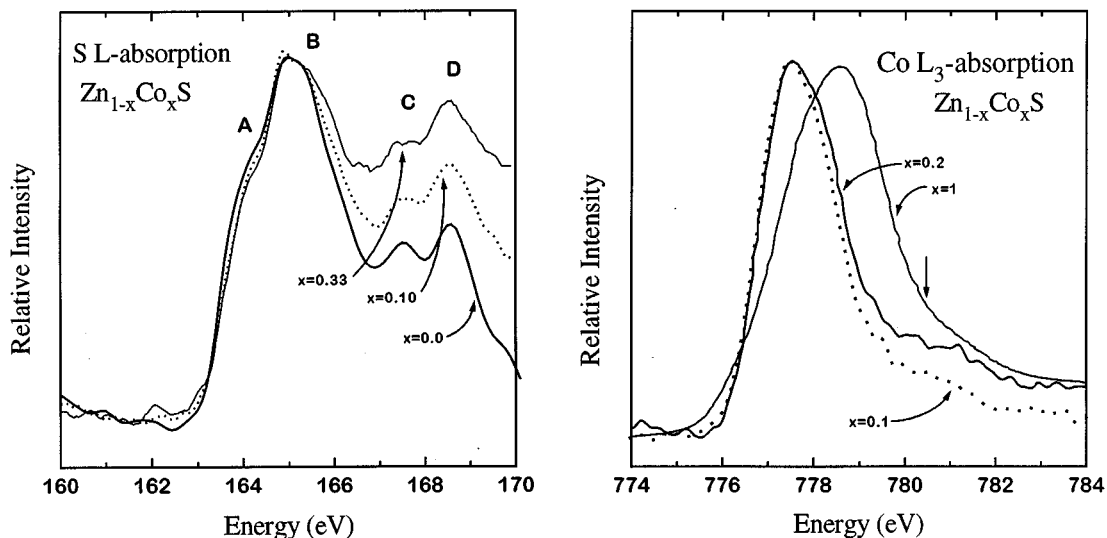


FIG. 3. The Co-L₃ spectra normalized at the maximum intensity, $x=0.1$ (dotted line), $x=0.2$ (bold line), $x=1.0$ (thin line), and the S-L_{2,3} absorption spectra normalized at the maximum intensity, $x=0.0$ (bold line), $x=0.1$ (dotted line), $x=0.3$ (thin line) of Zn_{1-x}Co_xS.

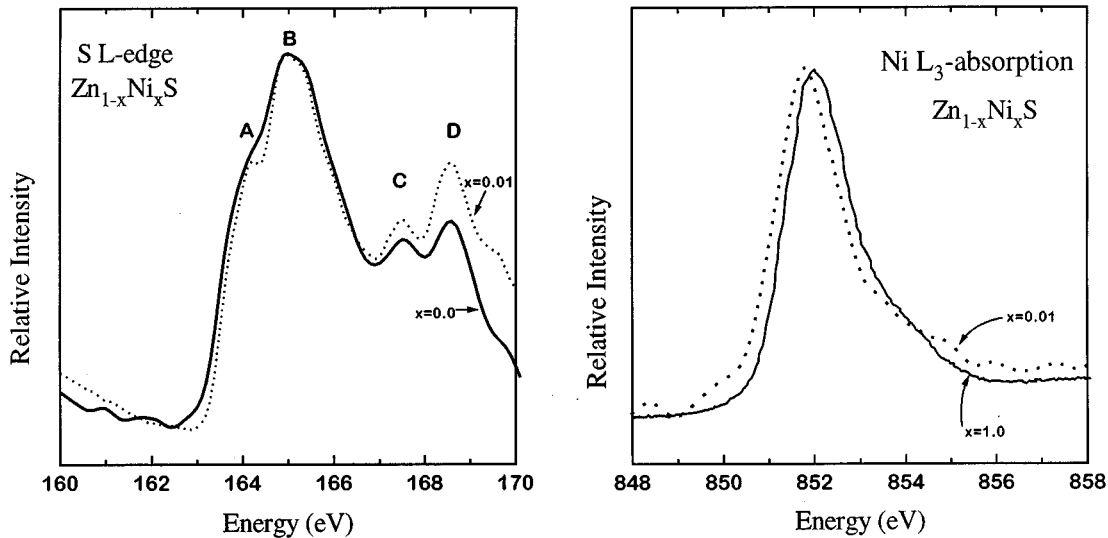


FIG. 4. The Ni-L₃ and the S-L_{2,3} absorption spectra normalized at the maximum intensity, $x=0.01$ (dotted line), $x=1.0$ (bold line) of $Zn_{1-x}Ni_xS$.

anion states. From EXAFS measurements,⁶ the Mn-S bond length R is 0.09 Å longer than the Zn-S bond in these DMS. Therefore, the direction of the energy shift of the S-L_{2,3} edges for the S atoms bonded to Mn is in agreement with the energy shifts suggested by the crystal field strength, which is proportional to $(1/R)^5$.

In Fig. 2, the Fe-L₃ and S-L_{2,3} absorption spectra from $Zn_{1-x}Fe_xS$ with $x=0.0, 0.11, 0.24, 0.34, 0.50$, and 1.0 are presented. As seen from Fe-L₃ absorption spectra, the 3d-4s antibonding states of Fe atoms are split into two subbands separated by about 1.7 eV. With the increase in Fe content, the energy separation of these subbands do not change. For the DMS with $x=0.5$, the intensity of high-energy subband reaches the maximum value (the subbands have almost equal intensity), suggesting that the Fe 3d states are concentrated at the second subband. The splitting of subbands depends on the Fe coordination and does not vary with Fe content. However, in the case of FeS, which is orthohedrally coordinated, the splitting is about 1.4 eV. The intensity distributions between the subbands depend on the Fe-Fe interatomic distance and thus on the overlapping of Fe 3d states.

In the case of S-L_{2,3} spectra presented in Fig. 2, we notice the appearance of an additional pre-edge structure indicated by an arrow. This structure was not observed in ZnS and the intensity of this feature increases with the concentration of Fe, indicating that there exists a direct hybridization of the 4s empty states of S with the 3d states of Fe and that the hybridized states are localized in the energy gap of host ZnS semiconductor. This may be responsible for the increase in conductivity of the $Zn_{1-x}Fe_xS$ with the increase of Fe content. Similar pre-edge structures have been observed in sulfur K absorption spectra.^{9,10} Additionally, changes in the higher-energy fine structure of the S-L absorption spectra that follow the changes in second subband of the Fe L edges (about 2 eV from the maximum of the edge) were also observed. As in the case of Mn, the 3d states of Fe participate in the forming of a bond of partial covalent character between the M and S.

In Fig. 3, the Co-L and S-L_{2,3} absorption spectra $Zn_{1-x}Co_xS$ for various Co concentrations ($x=0.0, 0.1, 0.2, 1.0$) are presented. The 3d-4s antibonding states of Co are accumulated in well localized bands with full width at half maximum of 2.0, 2.2, and 2.8 eV when $x=0.1, 0.2$, and 1.0, respectively. The small increase of the intensity at the high-energy side (indicated by an arrow) was detected, in spite of well pronounced subbands observed in Fe 3d states. The main absorption feature is much narrower (~ 1.0 eV) and shifted (~ 0.6 eV) to lower energy when compared to the main peak in orthohedrally coordinated CoS. With the increase in Co content, broadening of the main peak and increase in the intensity of the higher-energy feature was observed. In the case of S-L spectra, a small shift in energy (higher) as well as a decrease in intensity of peak A was observed. As in the case of Mn and Fe containing DMS, the intensity peaks B, C, and D increase with the Co content. In contrast to bond lengths of Mn-S and Fe-S, the bond length of Co-S bond is smaller than the bond length of Zn-S.⁵ This leads to an increase of the crystal field strength and therefore a shift of antibonding states of the sulfur atoms bonded to Co to a high energy. A small energy shift of the sulfur 2p doublet to a higher energy for S atoms bonded to Co was observed in the x-ray photoemission spectroscopy measurements.⁷ The 3d states of Co do not participate in the formation of the chemical bonding as much as the 3d states of Mn or Fe, but still some evidence of hybridization between Co and S states were discovered.

Examining the L edge absorption spectra in $Zn_{1-x}Ni_xS$ compounds presented in Fig. 4, only one peak formed by 3d antibonding states was observed. The width of this peak is the same for ternary and binary compounds indicating that these states do not participate in the chemical binding. About a 0.2 eV shift in energy of the edge position was observed. This is in agreement with the different coordination of the S atom in ternary and binary compounds. No pronounced changes at the site of sulfur atoms were observed.

The studies of the d and s antibonding states in $Zn_{1-x}M_xS$ compounds provide evidence that 3d states of

TABLE I. The chemical shift of transition metal K edges ΔE (eV) calculated from the theory of Kitamura and Chen²⁴ charge transfer $q(e)$ for $Zn_{1-x}M_xS$.

Energy of K edge for element (eV)	Compound	Chemical shift ΔE (eV)	Predicted charge $q(e)$
Mn 6539.0	$Zn_{1-x}Mn_xS$		
	$x=0.12$	8.0	2.46
	$x=0.20$	8.0	2.46
	$x=0.33$	8.0	2.46
error		0.1	± 0.05
Fe 7112.0	$Zn_{1-x}Fe_xS$		
	$x=0.11$	7.5	2.34
	$x=0.24$	7.8	2.37
	$x=0.50$	7.5	2.34
error		0.1	± 0.05
Co 7708.9	$Zn_{1-x}Co_xS$		
	$x=0.10$	7.3	2.30
	$x=0.16$	7.3	2.30
	$x=0.29$	7.3	2.30
error		0.1	± 0.05
Ni 8332.8	$Zn_{1-x}Ni_xS$		
	$x=0.01$	6.3	2.27
error		0.1	± 0.05
Zn 9658.6	ZnS		
		2.1	1.91
error		0.1	± 0.25

^aThe chemical shifts ΔE (eV) were estimated by subtracting the experimental K edge value (Ref. 9) of the metal E_0 in the alloys from the elemental metal K edge value.

transition metals participate in the formation of bonding (partial covalent) between M-S. Contrary to the p antibonding states in these materials⁹ the redistribution of the intensities between different $3d$ shell subbands with the increase of Mn and Fe content was observed. Nevertheless the level of hybridization between the transition metal atom and sulfur is different depending on the $3d$ orbit filling. The most pronounced changes in sulfur and metal absorption edges were observed for Mn and Fe containing compounds. The smallest evidence of hybridization was noticed for Co and Ni containing semiconductors.

X-ray absorption spectral features are sensitive to the chemical environment of the absorbing atoms under investigation.¹⁵ The change in the position of the main absorption edge, i.e., the chemical shift has been explained qualitatively based on the oxidation state,¹⁶ electronegativity,¹⁷ effective ionic charge,^{18,19} hybridization,^{17,20} ionicity,^{21,22} and the coordination number,²³ etc. Recently, for selected transition metals, Kitamura and Chen²⁴ have performed self-consistent calculations of the K-absorption edge energy and the chemical shift on the basis of the atomic nature, ignoring the effect of near-neighbor scattering potentials. Unlike the multiple scattering calculations, this method also limits the application mainly to ionic solids.

Based on the previously published chemical shift of the transition metal K edges,⁹ the calculated effective charge transfers in the cation-anion bond in $Zn_{1-x}M_xS$ in terms of

the theoretical approach of Kitamura and Chen²⁴ are presented in Table I. The chemical shifts for the particular metals in these compounds were found to be practically independent of the metal content. On the other hand, noticeable changes in chemical shift between the different transition metals in alloys were observed. The highest energy shift ($\Delta E=8.0$ eV) was found for Mn, whereas the lowest energy shift ($\Delta E=1.5$ eV) was found for Zn. The degree of ionicity of the partial covalent bond in ZnS is about 0.63, which is rather high.²⁵ This justifies estimating the effective cation charge q from the theoretical chemical shift at the K edges for different transition metal ions, M^{+q} .²⁴ For Zn we obtained a cation charge of $191e$ V, which is close to the formal value of $20e$ V. This provides a reasonable verification of the approximation used in Ref. 24 for $Zn_{1-x}M_xS$ compounds and that the contribution from the near-neighbor scattering potentials to the energy shifts in absorption threshold energy is small. The calculated charge values for different transition metals are greater than 2.0. This confirms our conclusions from L absorption edge measurements that in the case of transition metals, besides the electrons from $4sp$ orbitals, the $3d$ electrons also contribute to the overall charge transfer. As seen from Table I, when the atomic number is increased (from Mn to Ni), a decrease in charge transfer is observed in spite of the increase in number of $3d$ electrons. The $3d$ orbitals of Mn are only in half filled, but in the case of Ni, $3d$ orbitals are already almost completely filled ($3d^9$). The Zn $3d$ orbit are in a closed configuration and we do not find any evidence of Zn $3d$ electrons participating in ionic bonding.

IV. CONCLUSION

The near edge soft x-ray-absorption spectra from $Zn_{1-x}M_xS$ compounds, where M equals Mn, Fe, Co, and Ni, and x ranging from zero to the solubility limit, were measured with high resolution by measuring the total electron yield from the sample. The absorption spectra obtained by this method are not distorted by the inhomogeneity (roughness) of the sample, the so called thickness effect. The studies of d and s antibonding states in these compounds provided evidence that the $3d$ electrons of transition metals participate in the formation of partial covalent bonding between M-S and that the ability of $3d$ electrons to participate in ionic bonding decreases with an increase in $3d$ orbit filling. The more closed the $3d$ orbit of electrons are, the more corelike character the $3d$ electrons exhibit. Strong evidence of this behavior can be seen in the L absorption spectra of metal and sulfur and in the calculated charge transfer based on the chemical shifts in transition metal K edges. In the case of Mn and Fe, a very pronounced change in the shape of cation and anion L edges with the change in metal content was observed, whereas in the case of Co and Ni the effect was much smaller. This explains the dramatic decrease of the solubility of the investigated metals in the ZnS matrix for various cations. The solubility limit, which is $x=0.60$, in the case of Mn, decreases to $x=0.03$ when the cation is changed to Ni. An extension of this work is to measure the absolute near-edge absorption cross sections for these materials and to obtain the d -band occupancy from the white line areas.

ACKNOWLEDGMENTS

The crystals studied have been prepared by Dr. Z. Golacki, whose contribution is greatly acknowledged. One of the authors (K. L-J) kindly acknowledges the financial support of the Fulbright Foundation. This work was supported by the Office of Basic Energy Science of the Department of Energy under Contract No. DE-AC03-76SF00098.

*Present address: Institute of Physics, Polish Academy of Science, Al. Lotnikow 32/46, 02 668 Warsaw, Poland.

¹*Proceedings of the 5th International Conference on II-VI Compounds*, Tammano, 1992 (North-Holland, Amsterdam, 1992).

²*Proceedings of the 6th International Conference on II-VI Compounds*, Newport, RI, 1992 (North-Holland, Amsterdam, 1992).

³A. Balzarotti, N. Motta, A. Kisiel, M. Zimnal-Starnawska, M. T. Czyzyk, and M. Podgorny, *Phys. Rev. B* **31**, 7526 (1985).

⁴R. A. Mayanovic, W. F. Pong, and B. A. Bunker, *Phys. Rev. B* **42**, 11 174 (1990).

⁵K. Lawniczak-Jablonska and Z. Golacki, *Acta Phys. Pol. A* **86**, 727 (1994).

⁶R. J. Iwanowski, K. Lawniczak-Jablonska, I. Winter, and J. Hormes, *Solid State Commun.* **97**, 879 (1996).

⁷K. Lawniczak-Jablonska, Z. Golacki, W. Paszkowicz, J. Masek, L. -S. Johansson, and M. Heinonen, *J. Phys. Condens. Matter* **6**, 3369 (1994).

⁸L. Martinez, L. R. Ganzalez, and W. Giriat, *Phys. Status Solidi B* **180**, 267 (1995).

⁹K. Lawniczak-Jablonska, R. J. Iwanowski, Z. Golacki, A. Traverse, S. Pizzini, A. Fontaine, I. Winter, and J. Hormes, *Phys. Rev. B* **53**, 1119 (1996).

¹⁰W. F. Pong, R. A. Mayanovic, K. T. Wu, P. K. Tseng, B. A. Bunker, A. Hiraya, and M. Watanabe, *Phys. Rev. B* **50**, 7371 (1994).

¹¹A. Twardowski in *Diluted Magnetic Semiconductors*, edited by M. Jain (World Scientific, Singapore, 1991), p. 276.

¹²D. Li, G. M. Bancroft, M. Kasrai, M. E. Fleet, X. H. Feng, K. H. Tan, and B. X. Yang, *J. Phys. Chem. Solids* **55**, 535 (1994).

¹³J. H. Underwood, E. M. Gullikson, M. Koike, P. C. Batson, P. E. Denham, and R. Steele, *Rev. Sci. Instrum.* **67**, 1 (1996).

¹⁴W. R. L. Lambrecht, S. N. Rashkeev, B. Segall, K. Lawniczak-Jablonska, T. Suski, E. M. Gullikson, J. H. Underwood, R. C. C. Perera, J. C. Rife, I. Grzegory, S. Porowski, and D. K. Wickenden, *Phys. Rev. B* **55**, 2612 (1997).

¹⁵D. J. Nagel and W. L. Baum, in *X-Ray Spectroscopy*, edited by L. V. Azaroff (McGraw-Hill, New York, 1974), p. 445.

¹⁶A. K. Nigam and M. K. Gupta, *J. Phys. F* **3**, 1251 (1973).

¹⁷S. Kwata and K. Maeda, *J. Phys. C* **11**, 2391 (1978).

¹⁸J. P. Suchet and F. Bailly, *Anal. Chem.* **10**, 517 (1965).

¹⁹P. R. Sarode, S. Ramesha, W. H. Madhusudan, and C. N. R. Rao, *J. Phys. C* **12**, 2439 (1979).

²⁰V. G. Bhide and S. K. Kaicker, *J. Chem. Phys.* **35**, 695 (1974).

²¹A. K. Dey and B. K. Agarwal, *Nuovo Cimento Lett.* **1**, 803 (1971).

²²S. V. Adhyapak and A. S. Nigavekar, *J. Phys. Chem. Solids* **37**, 1037 (1976).

²³U. C. Srivastava and H. L. Nigam, *Coordination Chem. Rev.* **9**, 276 (1973).

²⁴M. Kitamura and H. Chen, *J. Phys. Chem. Solids* **52**, 731 (1991).

²⁵S. V. Adhyapak and A. S. Nigavekar, *J. Phys. Chem. Solids* **37**, 1037 (1976).